

Line-on-Line Coincidence: A New Type of Epitaxy Found in Organic-Organic Heterolayers

Stefan C. B. Mannsfeld, Karl Leo, and Torsten Fritz

Institut für Angewandte Photophysik, Technische Universität Dresden, D-01062 Dresden, Germany

(Received 27 August 2004; published 11 February 2005)

We propose a new type of epitaxy, *line-on-line coincidence* (LOL), which explains the ordering in the organic-organic heterolayer system PTCDA on HBC on graphite. LOL epitaxy is similar to point-on-line coincidence (POL) in the sense that all overlayer molecules lie on parallel, equally spaced lines. The key difference to POL is that these lines are not restricted to primitive lattice lines of the substrate lattice. Potential energy calculations demonstrate that this new type of epitaxy is indeed characterized by a minimum in the overlayer-substrate interaction potential.

DOI: 10.1103/PhysRevLett.94.056104

PACS numbers: 81.15.Aa, 61.66.Hq, 68.55.-a, 74.78.Fk

Organic semiconductors are actively investigated due to promising optoelectronic applications such as organic luminescence displays and solar cells [1,2]. Most of the devices realized so far use polycrystalline or even amorphous organic films. Highly ordered films, i.e., ultrathin organic molecular crystals, can provide deeper insight into the physical processes occurring in devices, but could also allow much better device performance: even small disorder reduces the mobility by many orders of magnitude [3]. The mechanism of highly ordered (epitaxial) overlayers in *inorganic-inorganic heteroepitaxy* (IIHE) is well understood, mainly due to the pioneering work of Frank and van der Merwe [4]. In the case of *organic-inorganic heteroepitaxy* (OIHE), the structure of the first monolayer usually depends on a delicate balance of weak noncovalent interactions between the molecules in the overlayer (i.e., the *intralayer* interactions) and between the overlayer and the substrate (i.e., the *interlayer* interactions). Compared to the scenario of IIHE, less obvious epitaxy modes occur in OIHE systems. Since most of the organic devices are based on heterojunctions, both OIHE and *organic-organic heteroepitaxy* (OOHE) are relevant. In particular, little is known about the latter.

The established classification scheme for OIHE [5] relies on the epitaxy matrix C relating primitive overlayer lattice basis vectors ($\mathbf{b}_1, \mathbf{b}_2$) to primitive basis vectors of the subjacent substrate surface lattice ($\mathbf{a}_1, \mathbf{a}_2$):

$$\begin{bmatrix} \mathbf{b}_1 \\ \mathbf{b}_2 \end{bmatrix} = C \cdot \begin{bmatrix} \mathbf{a}_1 \\ \mathbf{a}_2 \end{bmatrix} = \begin{bmatrix} C_{11} & C_{12} \\ C_{21} & C_{22} \end{bmatrix} \cdot \begin{bmatrix} \mathbf{a}_1 \\ \mathbf{a}_2 \end{bmatrix}. \quad (1)$$

The three epitaxy types described in Ref. [5] can be classified by the number of integer elements in the matrix C : (i) If all overlayer lattice points coincide with substrate lattice points, the overlayer is *commensurate*, and all C_{ij} matrix elements are integers. (ii) *Coincidence-I* or *point-on-line coincidence* (POL) is characterized by having all overlayer molecules lying on primitive lattice lines of the substrate surface lattice. This is indicated by one column of integer elements in the matrix C . (iii) Only a fraction of the overlayer lattice points of a *coincident-II* overlayer

coincides with substrate lattice points; i.e., the overlayer forms a supercell whose corner points are in registry with the substrate. All C_{ij} matrix elements are rational (no integer column in the matrix). (iv) If the overlayer lattice neither coincides with substrate lattice points nor primitive substrate lattice lines, the overlayer is denoted *incommensurate*.

In this Letter, we investigate an organic-organic heteroepitaxy system grown by organic molecular beam epitaxy (OMBE): A highly ordered layer of the planar aromatic molecule perylene-3,4,9,10-tetracarboxylic-3,4,9,10-dianhydride (PTCDA) is grown on top of a monolayer of a second planar aromatic molecule, perihexabenzocoronene (HBC). HBC was deposited beforehand, forming a commensurate ($\sqrt{31} \times \sqrt{31}$) $R8.9^\circ$ lattice with the graphite(0001) substrate [6,7]. Scanning tunneling microscopy (STM) images show smooth layers of flat lying PTCDA molecules [7] and a characteristic moiré pattern (Fig. 1). We performed an evaluation of this moiré pattern yielding highly precise [8] PTCDA unit cell dimensions (Table I). The simulated moiré pattern [Fig. 1(c)] is created by a superposition of the point lattices of PTCDA and HBC ($\phi = 10.0^\circ$ orientation of PTCDA from Table I) and fits very well to the experiment [Fig. 1(b)].

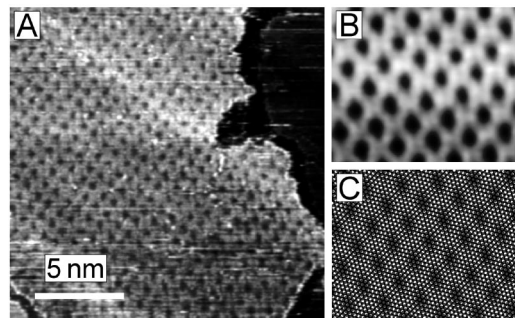


FIG. 1. (a) STM image of PTCDA on HBC on graphite [$V = 0.93$ V, $I = 0.11$ nA]. (b) A zoomed portion of the experimentally observed moiré pattern is shown to the right; (c) the simulated moiré pattern is depicted beneath.

TABLE I. Dimensions and orientations of the PTCDA lattice on HBC on graphite as determined by a moiré pattern analysis of the results from Ref. [7]. Here, \mathbf{b}_1 and \mathbf{b}_2 denote the PTCDA unit cell vectors, Γ is the PTCDA unit cell angle, and $\phi = \angle(\mathbf{b}_1, [\bar{1}2\bar{1}0]_{\text{Graph}})$ defines the PTCDA domain angle (see Fig. 2).

$ \mathbf{b}_1 $ (Å)	$ \mathbf{b}_2 $ (Å)	Γ (deg)	ϕ (deg)	C matrix
12.28	19.48	90.0	10.0	$\begin{pmatrix} 0.886 & 0.019 \\ -0.847 & 1.641 \end{pmatrix}$
12.28	19.48	90.0	-10.0	$\begin{pmatrix} 1.015 & -0.336 \\ -0.315 & 1.552 \end{pmatrix}$

Surprisingly, the epitaxy matrices from Table I correspond to incommensurate alignments between the PTCDA lattice and the HBC lattice, despite the observation of the moiré pattern which is direct proof of ordering. To resolve this discrepancy, we propose here a new type of epitaxy which we denote *line-on-line coincidence* (LOL). The LOL epitaxy explains the observed experimental results and is assumed to be of general importance in OOHE systems. This new type of epitaxy is characterized by a coincidence between *nonprimitive* reciprocal lattice vectors of the overlayer and the substrate. A key property of an epitaxial alignment between two lattices is a minimum in the interlayer interaction potential V_{inter} between the first and the second layer. This holds true in the case of IIHE [9–12] as well as for OIHE [13–15]. The results of potential energy (PE) calculations presented in the following demonstrate that this new type of epitaxy is also marked by a minimum in V_{inter} , with the subsystem HBC layer/graphite being regarded as the substrate.

Several attempts have been made to predict epitaxial alignments of thin films [13,15–18]. PE based models typically rely on three assumptions: (i) Only two-body additive interactions are considered. (ii) The V_{inter} value is calculated as the sum of an atom-atom potential over all atoms in the interface. (iii) The substrate is assumed to be rigid. Here, this assumption can also be made for the adsorbate molecules. However, it is computationally too tedious to perform PE calculations for realistically large overlayer domains comprising several thousand molecules, even if these assumptions are employed. Therefore, we use a highly efficient approach which we especially developed for flat lying molecules [15]. Here, we use a Lennard-Jones potential in conjunction with the parameters from the optimized potentials for liquid simulations force field [19].

The investigated scenario is schematically depicted in Fig. 2. There, \mathbf{a}_1 denotes one unit cell vector of the hexagonal $(\sqrt{31} \times \sqrt{31})R8.9^\circ$ HBC lattice, and Δ describes the position of the PTCDA lattice relative to the HBC lattice. The arrangement of the two PTCDA molecules in the unit cell is very similar to the (102) bulk plane. However, it could not be precisely determined by STM analysis. Therefore, we used the values from the β -PTCDA bulk crystal [20] [molecules projected onto the (102) plane] for

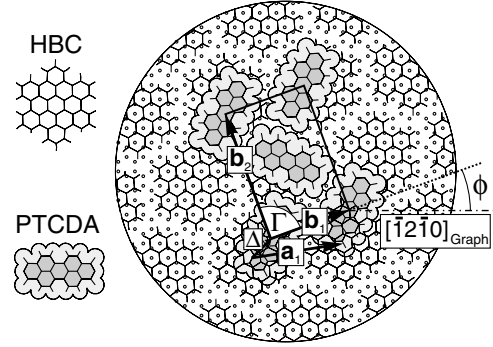


FIG. 2. Schematic representation of the PE curve calculation procedure for PTCDA on HBC on graphite. In order to evaluate the V_{inter} potential combined with the different PTCDA domain orientations, a large PTCDA domain (two molecules per unit cell) is rotated with respect to the HBC/graphite substrate system.

the PE calculations. The model substrate considered for each PTCDA molecule consisted of 34 HBC molecules arranged in a $(\sqrt{31} \times \sqrt{31})R8.9^\circ$ lattice on top of a circular two-layer graphite(0001) crystal with >6000 atoms.

Figure 3 shows the overlayer-substrate potential V_{inter} as a function of the domain angle ϕ for differently sized circular PTCDA domains with fixed unit cell dimensions (Table I). For a meaningful comparison of different orientations, the lateral position Δ of the PTCDA domain was optimized for each domain angle. The vertical separation between the PTCDA domains and the HBC layer was kept fixed at the precalculated optimum value of 3.43 Å. The right y axis is labeled *energetic gain per molecule*, which refers to the difference between the PE values of the current PTCDA domain orientation and the energetically highest PTCDA domain orientation (incommensurate alignment), divided by the number of molecules in the domain. It can be seen that the V_{inter} potential exhibits

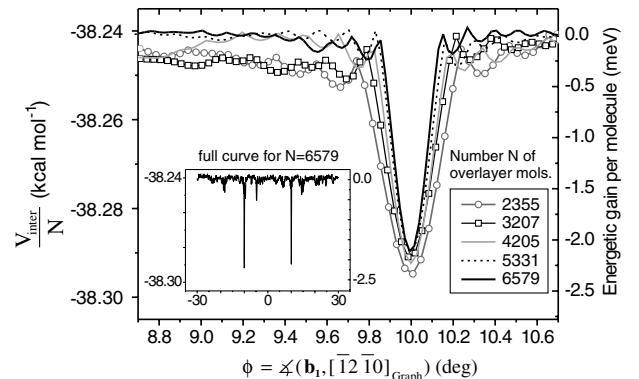


FIG. 3. Dependence of the interlayer potential V_{inter} on the PTCDA domain orientation ϕ , calculated for differently sized PTCDA domains on HBC on graphite. The domain diameter varies in the range: 60–100 nm (2355–6579 PTCDA molecules). The lower-left inset shows the 100 nm curve across the full investigated range of angles.

distinct minima exactly at the experimental domain angles (see Table I). Furthermore, the energetic gain per molecule at these domain angles converges to a constant value of ~ 2.2 meV with increasing domain size (only shown for $\phi = 10.0^\circ$), while the minimum gets narrower at the same time. These properties indicate that the respective minimum-potential domain orientations correspond to coherent, i.e., epitaxial, alignments between the overlayer and the substrate lattice [10,14,15].

We now exemplarily discuss the lateral corrugation of the V_{inter} potential for the $\phi = 10.0^\circ$ orientation. Thus, a V_{inter} potential map is calculated by variation of the PTCDA domain position vector Δ (Fig. 4). The map exhibits a 1D periodicity (vector \mathbf{p}) with a corrugation of $0.13 \text{ kcal mol}^{-1}$ (5.4 meV). If the PTCDA domain is rotated from the $\phi = 10.0^\circ$ orientation by only 2° , the corrugation depth drops by almost 2 orders of magnitude. Similar 1D potential patterns were obtained previously for POL PTCDA domains on graphite [15]. Furthermore, both the HBC and the PTCDA unit cell span an integer number of periods of this 1D potential pattern at the $\phi = 10.0^\circ$ orientation:

$$\mathbf{p} \cdot \mathbf{a}_1 = 1|\mathbf{p}|^2, \quad \mathbf{p} \cdot \mathbf{a}_2 = 6|\mathbf{p}|^2, \quad (2)$$

$$\mathbf{p} \cdot \mathbf{b}_1 = 1|\mathbf{p}|^2, \quad \mathbf{p} \cdot \mathbf{b}_2 = 9|\mathbf{p}|^2. \quad (3)$$

Equations (2) and (3) can only be satisfied at the same time if the following nonprimitive reciprocal PTCDA and HBC lattice vectors coincide: $\mathbf{b}_1^* + 9\mathbf{b}_2^* = \mathbf{a}_1^* + 6\mathbf{a}_2^*$. The other minimum-potential PTCDA domain orientation $\phi = -10^\circ$ exhibits a very similar coincidence of reciprocal lattice vectors: $-\mathbf{b}_1^* + 9\mathbf{b}_2^* = \mathbf{a}_1^* + 6\mathbf{a}_2^*$. Hence, the $\phi = \pm 10.0^\circ$ orientations of PTCDA on HBC involve lattice match, but between the respective *reciprocal* lattice vectors $i\mathbf{b}_1^* + j\mathbf{b}_2^* = k\mathbf{a}_1^* + l\mathbf{a}_2^*$ (and all multiples of these) instead of real space lattice vectors. We denote this new epitaxy type line-on-line coincidence because in real space

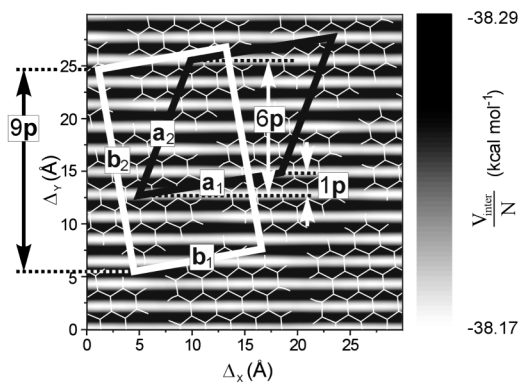


FIG. 4. V_{inter} potential map calculated by the lateral translation of a 50 nm PTCDA domain (1649 molecules) at a domain angle of $\phi = 10.0^\circ$ on the HBC/graphite substrate. The potential surface exhibits a 1D pattern. The hexagonal HBC unit cell (black) as well as the rectangular PTCDA unit cell (white) span integer numbers of periods (vector \mathbf{p}) of this 1D pattern.

the $[ij]$ -lattice lines of the overlayer coincide with the $[kl]$ -lattice lines of the substrate. Similar to POL, all molecules of a LOL overlayer lie on lattice lines of the substrate (see Fig. 4). However, the important difference between LOL and POL is that in the case of POL these lines are restricted to primitive lattice lines of the substrate surface lattice; i.e., one of the integer coefficients k and l would have to be 1, the other 0.

The importance of treating epitaxy in reciprocal space was previously highlighted for IIHE systems by Braun *et al.* [21]. Assuming an infinitely extended rigid substrate lattice and zero temperature, the V_{inter} potential can be written as the Fourier series:

$$V_{\text{inter}} = \sum_{\mathbf{G}} \varphi_{\mathbf{G}} \sum_{\{\mathbf{L}\}} e^{2\pi i \mathbf{G} \mathbf{L}}. \quad (4)$$

In Eq. (4), $\mathbf{G} = k\mathbf{a}_1^* + l\mathbf{a}_2^*$ are the reciprocal substrate lattice vectors, $\varphi_{\mathbf{G}}$ the Fourier coefficients. The overlayer domain is represented by a set $\{\mathbf{L}\}$ of N overlayer lattice vectors, and a corresponding set of reciprocal lattice vectors $\{\tau\}$. The term $\sum_{\{\mathbf{L}\}} e^{2\pi i \mathbf{G} \mathbf{L}}$ is called the *lock-in term* and depends on the mutual alignment of the point lattices of the overlayer and the substrate only; i.e., geometrical lattice match/mismatch is exclusively contained in the lock-in term. It exhibits sharp maxima where \mathbf{G} coincides with a τ vector. In the limit of an infinitely extended overlayer domain ($N \rightarrow \infty$), the lock-in term converges towards a Dirac delta function $\delta(\mathbf{G} - \tau)$. Therefore, apart from $\varphi_{\mathbf{G}=0}$, which represents the incommensuration energy, only those Fourier coefficients $\varphi_{\mathbf{G}}$ which fulfill the coincidence condition $\mathbf{G} = \tau$ are actually added to the V_{inter} sum expression in Eq. (4).

In contrast to the new epitaxy type reported here, all types of epitaxy which occur in IIHE or in OIHE are characterized by coincidences of *primitive* reciprocal substrate lattice vectors \mathbf{G} with reciprocal lattice vectors τ of the overlayer, hence there is always a visible lattice match in real space. Furthermore, there is a *single* potential minimum (for an adsorbate particle) per substrate lattice unit cell in these cases. The OOHE scenario is fundamentally different insofar as a single substrate lattice unit cell possesses a complex inner structure. This important difference can be highlighted by discussing the algebraic structure of the Fourier coefficients from Eq. (4):

$$\varphi_{\mathbf{G}} = \frac{e^{2\pi i \mathbf{G} \Delta}}{V_{\text{Cell}}} \int_{V_{\text{Cell}}} d\mathbf{r} \varphi(\mathbf{r}) e^{-2\pi i \mathbf{G} \mathbf{r}}. \quad (5)$$

In Eq. (5), V_{Cell} denotes the area of a substrate unit cell, while the potential function $\varphi(\mathbf{r})$ is the V_{inter} potential of a single overlayer unit cell (two PTCDA molecules) as a function of its position \mathbf{r} within the area of the substrate unit cell. Figure 5 shows the $\varphi(\mathbf{r})$ function, calculated for the $\phi = 10.0^\circ$ orientation of PTCDA on HBC. It can be seen that $\varphi(\mathbf{r})$ exhibits *multiple* local minima within the area of a HBC unit cell (white).

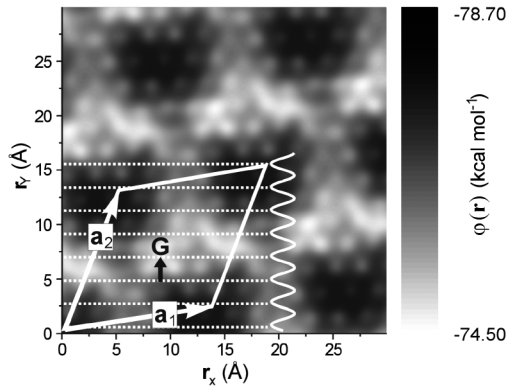


FIG. 5. The potential function $\varphi(\mathbf{r})$ for the case of PTCDA on HBC at a domain angle of $\phi = 10.0^\circ$. The reciprocal substrate lattice vector \mathbf{G} (the corresponding plane wave is sketched by dotted lines) gives rise to a resonance in the Fourier series.

Under the integral in Eq. (5), $\varphi(\mathbf{r})$ is multiplied with a plane wave term $e^{-2\pi i \mathbf{G} \cdot \mathbf{r}}$. This plane wave term effectively “probes” the periodicity of the potential $\varphi(\mathbf{r})$, whereas the frequency and the direction of the probing wave are determined by the vector \mathbf{G} . Therefore, if there is only a single minimum within the area of a substrate unit cell as in the cases of IIHE and OIHE, the higher order Fourier coefficients $\varphi_{\mathbf{G}}$ quickly converge towards zero with increasing $|\mathbf{G}|$. Hence coincidence of first order \mathbf{G} vectors with τ vectors gives rise to minima in V_{inter} . In case of OOHE, resonant higher order terms of the Fourier series can occur, depending on the energetic “topology” $\varphi(\mathbf{r})$ within the substrate unit cell. These terms can establish the dominant contribution to the V_{inter} potential, if the respective reciprocal substrate lattice vector \mathbf{G} coincides with a reciprocal overlayer lattice vector. Here, the nonprimitive reciprocal substrate lattice vector $\mathbf{G} = \mathbf{a}_1^* + 6\mathbf{a}_2^*$ creates such a resonance (by coinciding with $\tau = \pm \mathbf{b}_1^* + 9\mathbf{b}_2^*$) which leads to the V_{inter} minima at $\phi = \pm 10.0^\circ$. The respective plane wave is depicted by dotted lines in Fig. 5. The wavelength $\frac{1}{|\mathbf{G}|}$ (1D periodicity of the potential surface in Fig. 4) is identical to a characteristic distance in a graphite(0001) surface lattice: $2.1313 \text{ \AA} = \frac{\sqrt{3}}{2} \times 2.461 \text{ \AA}$. Therefore, it can be concluded that the graphitic subunits of the HBC molecules are responsible for this higher order resonance. However, we can rule out the possibility that the subjacent graphite(0001) crystal has a significant influence on the PTCDA film structure since PE calculations that were performed without the graphite crystal yielded qualitatively similar results. The fact that it is essential to consider higher order Fourier terms also provides a lucid explanation for the missing capability of pseudopotential-based epitaxy prediction methods [13,14] to detect such epitaxial alignments between the overlayer and the substrate. The use of sinusoidal functions as a model for the V_{inter} poten-

tial corresponds to a consideration of only first order terms of the Fourier series.

In conclusion, we have demonstrated that the film structure of PTCDA on HBC on graphite corresponds to a new type of epitaxy which is characterized by a coincidence between overlayer lattice lines and nonprimitive substrate lattice lines. The characteristic difference to the already known epitaxy types is the existence of resonant higher order Fourier coefficients in the Fourier series representation of the interface potential, induced by the inner structure of the substrate lattice unit cell.

We acknowledge DFG Grants No. FOR 335/2-1, No. LE 747/24-4, and No. FR 875/6.

- [1] L. S. Hung and C. H. Chen, Mater. Sci. Eng., R **39**, 143 (2002).
- [2] P. Peumans, A. Yakimov, and S. R. Forrest, J. Appl. Phys. **93**, 3693 (2003).
- [3] N. Karl and J. Marktanner, Mol. Cryst. Liq. Cryst. **355**, 149 (2001).
- [4] F. C. Frank and J. H. van der Merwe, Proc. R. Soc. London A **198**, 205 (1949).
- [5] D. E. Hooks, T. Fritz, and M. D. Ward, Adv. Mater. **13**, 227 (2001).
- [6] C. Günther, *Organische Molekularstrahlepitaxie: Ordnungsprinzipien großer Aromaten auf Schichtalbleitern* (LOGOS Verlag, Berlin, 1998).
- [7] T. Schmitz-Hübsch *et al.*, Surf. Sci. **445**, 358 (2000).
- [8] A change of the PTCDA lattice constants by only $\pm 0.01 \text{ \AA}$ leads to unacceptable deviations between measured and simulated moiré lattice.
- [9] J. H. van der Merwe and M. W. H. Braun, Appl. Surf. Sci. **22/23**, 545 (1985).
- [10] A. Kobayashi and S. Das Sarma, Phys. Rev. B **35**, 8042 (1987).
- [11] S. M. Paik and I. K. Schuller, Phys. Rev. Lett. **64**, 1923 (1990).
- [12] A. Catana, J.-P. Locquet, S. M. Paik, and I. K. Schuller, Phys. Rev. B **46**, 15477 (1992).
- [13] A. C. Hillier and M. D. Ward, Phys. Rev. B **54**, 14037 (1996).
- [14] J. A. Last, D. E. Hooks, A. C. Hillier, and M. D. Ward, J. Phys. Chem. B **103**, 6723 (1999).
- [15] S. C. B. Mannsfeld and T. Fritz, Phys. Rev. B **69**, 75416 (2004).
- [16] J. P. McTague and A. D. Novaco, Phys. Rev. B **19**, 5299 (1979).
- [17] F. Grey and J. Bohr, Europhys. Lett. **18**, 717 (1992).
- [18] S. R. Forrest, P. E. Burrows, E. I. Haskal, and F. F. So, Phys. Rev. B **49**, 11309 (1994).
- [19] W. Damm, A. Frontera, J. Tirado-Rives, and W. L. Jorgensen, J. Comput. Chem. **18**, 1955 (1997).
- [20] T. Ogawa *et al.*, Acta Crystallogr. Sect. B **55**, 123 (1999).
- [21] M. W. H. Braun, H. S. Kong, J. T. Glass, and R. F. Davis, J. Appl. Phys. **69**, 2679 (1991).